

Cascade of magnetic-field-induced quantum phase transitions in a spin $\frac{1}{2}$ triangular-lattice antiferromagnet

N. A. Fortune,¹ S. T. Hannahs,² Y. Yoshida,^{3,*} T. E. Sherline,^{3,†} T. Ono,⁴ H. Tanaka,⁴ and Y. Takano³

¹*Department of Physics, Smith College, Northampton, MA 01063, USA*

²*National High Magnetic Field Laboratory, 1800 E. Paul Dirac Dr., Tallahassee, FL 32310, USA*

³*Department of Physics, University of Florida, P.O. Box 118440, Gainesville, Florida 32611-8440, USA*

⁴*Department of Physics, Tokyo Institute of Technology, Meguro-ku, Tokyo 152-8551, Japan*

(Dated: November 8, 2018)

We report magnetocaloric and magnetic-torque evidence that in Cs_2CuBr_4 — a geometrically frustrated Heisenberg $S = \frac{1}{2}$ triangular-lattice antiferromagnet — quantum fluctuations stabilize a series of spin states at simple increasing fractions of the saturation magnetization M_s . Only the first of these states — at $M = \frac{1}{3}M_s$ — has been theoretically predicted. We discuss how the higher fraction quantum states might arise and propose model spin arrangements. We argue that the first-order nature of the transitions into those states is due to strong lowering of the energies by quantum fluctuations, with implications for the general character of quantum phase transitions in geometrically frustrated systems.

PACS numbers: 75.30.Kz, 75.40.Cx, 75.50.Ee

Geometric frustration appears in a wide variety of physical systems [1, 2, 3]. In a classical system, this frustration leads to a large number of states of identical energy. Quantum fluctuations can lift this degeneracy, creating classically unexpected ground states and excitations.

For one of the simplest possible frustrated systems—a Heisenberg antiferromagnet with spins of quantum number $S = \frac{1}{2}$ arranged on a triangular lattice—theory predicts that quantum fluctuations should stabilize a novel up-up-down (*uud*) ground state [4, 5, 6]. Because this collinear state preserves the continuous rotation symmetry of the spin hamiltonian, low-energy excitations are separated from the ground state by energy gaps, resulting in the ground state of constant magnetization equal to $\frac{1}{3}$ of the saturation magnetization M_s over a finite field range. Experimentally, however, Cs_2CuBr_4 is the only known $S = \frac{1}{2}$ triangular-lattice antiferromagnet in which this up-up-down state occurs [7, 8, 9]. The suppression of this quantum stabilized state with increasing in-plane anisotropy prevents its formation in the isomorphic compound Cs_2CuCl_4 [5, 6].

The spin hamiltonian for Cs_2CuBr_4 is given by

$$\mathcal{H} = J_1 \sum_{\langle i,j \rangle} \vec{S}_i \cdot \vec{S}_j + J_2 \sum_{\langle i,k \rangle} \vec{S}_i \cdot \vec{S}_k, \quad (1)$$

where $J_1 = 11.3\text{K}$ for nearest-neighbor coupling along the b axis and $J_2 = 8.3\text{K}$ for weaker nearest-neighbor coupling within the bc plane [10]. Not included in the hamiltonian are two small perturbations expected to be present: an antiferromagnetic interlayer coupling that causes the spins to order at 1.4 K in zero field, and an anisotropic superexchange interaction (Dzyaloshinskii-Moriya) that causes the spins to lie along the plane of the triangular lattice at zero field. The Dzyaloshinskii-Moriya interaction is also likely responsible for the sup-

pression of the up-up-down transition in fields applied along the a axis (perpendicular to the triangular lattice) in Cs_2CuBr_4 . In Cs_2CuCl_4 , each of these is about 5% of J_1 [11].

Here we report the complete high-field phase diagram of Cs_2CuBr_4 up to the saturation magnetic field $H_s = 28.5\text{T}$. The phase diagram was established through a combination of magnetocaloric and magnetic-torque measurements. In addition to the expected ordered antiferromagnetic phase at $\frac{M}{M_s} = \frac{1}{3}$, we find a theoretically unexpected cascade of additional ordered antiferromagnetic phases at higher fractions of M_s .

The magnetocaloric experiment employed a miniature sample-in-vacuum calorimeter [12] inserted into the mixing chamber of a dilution refrigerator. Inside the calorimeter, the 5.35 mg sample was directly mounted on a $0.5\text{mm} \times 1\text{mm} \times 50\mu\text{m}$ ruthenium-oxide resistance thermometer with a minimum amount of nail polish. The sample and thermometer were weakly thermally linked via $25\mu\text{m}$ diameter phosphor-bronze wires to a sapphire ring embedded in a 7.0 mm diameter silver platform serving as the thermal reservoir. These wires also served as the electrical leads to the sample thermometer and mechanical support for the sample and thermometer.

When the magnetic field—produced by a 33 T resistive magnet and applied along the crystallographic c axis [13] of the sample—is slowly swept up or down, the magnetocaloric effect produces a temperature difference ΔT between the sample and the thermal reservoir that depends on the heat capacity C_H , the temperature dependence of the magnetization $(\partial M/\partial T)_H$, the field sweep rate \dot{H} , and the weak link’s thermal conductance κ [14]:

$$\Delta T = -\frac{T}{\kappa} \left[\left(\frac{\partial M}{\partial T} \right)_H + \frac{C_H}{T} \frac{d(\Delta T)}{dH} \right] \dot{H}. \quad (2)$$

Reversing the field sweep direction reverses the sign

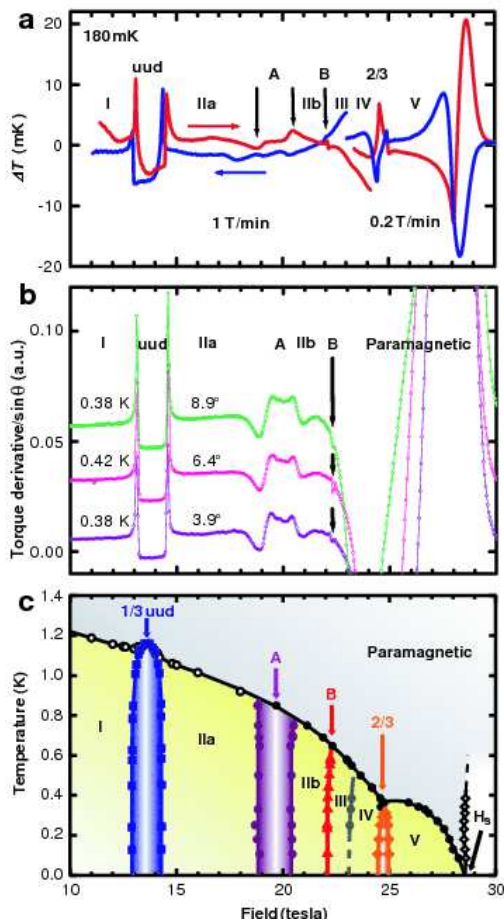


FIG. 1: (Color online) (a) Evolution of the temperature difference between the sample and thermal reservoir due to the magnetocaloric effect at 180 mK, with arrows indicating the field-sweep directions. (b) Derivative of magnetic torque with respect to H at temperatures near 400 mK. To produce a torque, the magnetic field was slightly tilted away from the c axis toward the b axis, by the angle indicated for each curve. (c) Magnetic phase diagram deduced from the magnetocaloric-effect data taken at various temperatures. Circles indicate second-order phase boundaries, whereas other symbols except the open diamonds indicate first-order boundaries. Open diamonds are the positions of the large features near H_s and do not indicate a phase boundary. Lines are guides to the eye. Data for $H \leq 18$ T are from Ref. [10], where open circles are from specific heat.

of the temperature difference, thereby revealing the sign and magnitude of $(\partial M/\partial T)_H$. Transitions between phases appear as deviations from a smoothly varying ΔT . First-order phase transitions will also reveal the release/absorption of latent heat as the sample enters/leaves a lower entropy state. At sufficiently low temperatures, there will also be an additional heat release as a metastable state gives way to the lower energy stable state for both field-sweep directions through a first-order transition.

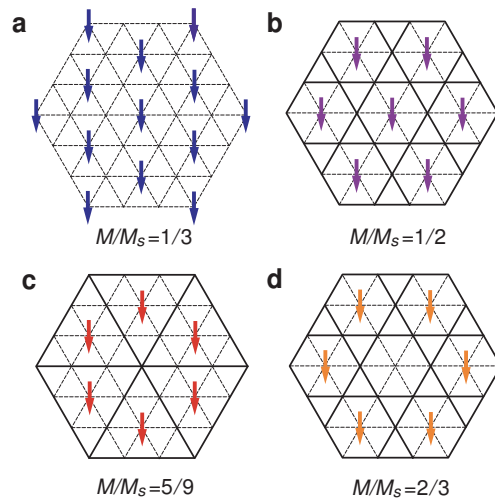


FIG. 2: (Color online) Collinear states on the triangular lattice at $M/M_s = \frac{1}{3}$, $\frac{1}{2}$, $\frac{5}{9}$, and $\frac{2}{3}$. Arrows indicate down spins antiparallel to the magnetic field. Vertices with no arrows indicate up spins pointing in the direction of the field, with broken lines marking rows containing both spins and solid lines marking rows of only up spins. The A phase may resemble the $M/M_s = \frac{1}{2}$ state, albeit not collinear.

Magnetocaloric-effect measurements can be made using swept fields [14], stepped fields [15], or modulated fields [16]. The resolution and reproducibility of dc field magnetocaloric measurements have traditionally been limited by temperature fluctuations, drift, and slow thermal response, all requiring high sweep rates producing additional heating. In this experiment, we have overcome these challenges to swept-field measurements through actively stabilizing the temperature of the thermal reservoir (sapphire/silver platform), minimizing the heat capacity of the addenda, and reducing the thermal relaxation time to less than 1 second. The reservoir temperature was maintained at a constant true temperature using the algorithm outlined in Ref. [17] to correct for the magnetoresistance of the sensor.

Magnetic phase transitions appear as anomalies in the sample temperature as shown in Fig. 1a. The phase diagram deduced from our magnetocaloric-effect data is shown in Fig. 1c, along with phase boundaries for fields $H \leq 18$ T from Ref. [10]. Additional evidence for this diagram is provided by the magnetic-torque data shown in Fig. 1b. Even for $S = \frac{1}{2}$ spins, theory has long assumed that the field region above the uud phase contains only one coplanar phase [4], at least for the isotropic Heisenberg hamiltonian. We find instead a remarkable cascade of phases in this field region. The boundaries between these ordered phases are nearly vertical, indicating that the phase diagram is primarily determined by the zero-temperature energies, not the entropies, of different states. We are witnessing a cascade of quantum

phase transitions.

The *uud* “plateau” phase appears in the field range 12.9 T–14.3 T [7, 8, 9, 10]. Below it is phase I, which is known to be incommensurate [8, 9, 18]. Above it lies phase IIa, which is also incommensurate but distinct from phase I [18]. The transitions between the *uud* phase and phases I and IIa are first-order [8, 9, 10, 19] and the low-lying excitations in this phase are gapped [10, 19].

In the field range 18.8 T–20.4 T, a new phase appears, the A phase. As seen in Figs. 1a and b, the transitions to it from phases IIa and IIb are second-order. Phase IIb, in the field range 20.4 T–22.1 T, may in fact be the same as phase IIa.

The magnetization of the A phase corresponds to roughly $\frac{1}{2}$ of the saturation magnetization but forms no plateau [8], suggesting that this phase is close to being collinear but is gapped. One likely arrangement for the nearby collinear state consists of alternating rows of up-down spins and only up spins, as depicted in Fig. 2b, an arrangement predicted to be the $M/M_s = \frac{1}{2}$ ground state of a triangular-lattice ring-exchange model for two-dimensional solid ^3He [20].

The most peculiar of all the new phases is the B phase, appearing at 22.1 T and only 70 mT wide. As seen in Fig. 1a, the transitions between the B phase and phases IIb and III are first-order. Like the A phase, the B phase can be recognized in retrospect as a small feature in the magnetic induction measured in pulsed magnetic fields [8]. Unlike the A phase feature, however, the feature of the B phase is pointed, suggesting a magnetization plateau and thus a collinear state with gapped low-lying excitations, at approximately $\frac{5}{9}$ of M_s .

Generalization of Lieb-Schultz-Mattis theorem [21] predicts that any gapped, ordered state must be commensurate [22, 23, 24]. Indeed, NMR of ^{133}Cs shows that the B phase is commensurate [25]. The collinearity and commensuratens suggest that the B phase may be the $\frac{5}{9}$ state depicted in Fig. 2c, a repetition of two rows of *uud* spins and one row of all up spins. Quantum calculations of the energy of this $\frac{5}{9}$ state have not yet been performed, but classically, this state is higher in energy than the coplanar and canted-spiral, three-sublattice states. Therefore, it is most likely that this new collinear, commensurate phase at $\frac{5}{9}$ of M_s — like the previously known collinear, commensurate phase at $\frac{1}{3}$ of M_s — owes its existence to strong quantum fluctuations.

Phase III, in the field region 22.1 T–23.1 T, is similar to phases IIa and IIb according to the magnetocaloric effect, implying that it is also incommensurate. The shapes of the boundaries between the B phase and phases IIb and III indicate that phase IIb is higher, whereas phase III is lower, in entropy than the B phase.

Phase IV directly borders on phase III at a second-order transition line. The boundary between this phase and the high-temperature, paramagnetic phase extrapolates to at most 26 T at zero temperature, well short of

$H_s = 28.5$ T. This surprising behavior indicates that the ground state of phase IV is higher in energy than a highly polarized, quantum-mechanically disordered state in the region starting from at least 26 T and extending to H_s .

The $\frac{2}{3}$ -magnetization-plateau phase [8] is observed here in the field region 24.5 T–25.0 T. The boundaries between this phase and phases IV and V are first-order. The requirement of collinearity and commensuratens for ordered magnetization-plateau states implies that the ground state of this phase should be an arrangement such as shown in Fig. 2d. Exact diagonalization for small systems shows that the ground state at $M/M_s = \frac{2}{3}$ is indeed collinear, for $0.5 \lesssim J_2/J_1 \lesssim 0.8$ [26]. Classically, this $\frac{2}{3}$ state is, like the lower fractional states, higher in energy than the coplanar and canted-spiral, three-sublattice states. Stabilization of the commensurate, collinear $\frac{2}{3}$ state observed here appears to imply the existence of large quantum fluctuations capable of significantly lowering the energy of this state below its classical expectation.

Phase V covers the highest field region up to H_s . In this phase, the magnetization increases steeply with increasing field [8], suggesting very rapid suppression of quantum fluctuations by the increasing field. The shape of the transition line between phase V and the paramagnetic phase is unlike all others in Fig. 1c, exhibiting slightly re-entrant behavior at about 25 T. These two features suggest that the phase is quite different from phases I–IV. One possibility is that this is a canted spiral phase.

Near H_s , the sample temperature exhibits a large peak during an upward field sweep and a deep dip during a downward sweep (Fig. 1a). They indicate a rapid change of entropy with magnetic field, signifying the emergence of a magnon energy gap at H_s .

The unexpected cascade of ordered phases within the antiferromagnetic phase boundary of Cs_2CuBr_4 is quite unlike the simple phase diagram of the semiclassical, spin- $\frac{5}{2}$, triangular-lattice antiferromagnet $\text{RbFe}(\text{MoO}_4)_2$ [27]. The strong contrast demonstrates that even the simplest model of geometrically frustrated antiferromagnetic interactions is much richer than previously imagined, when it is governed by quantum mechanics, with important implications for many current theoretical models of superconductivity and magnetism.

One important implication is, of course, the prospect of new, as yet undiscovered quantum states in such models, but a second is that the transitions to these states are commonly first order. The transitions to all three gapped phases observed here—the *uud* phase at $\frac{1}{3}$ M_s , the very narrow B phase at $\frac{5}{9}$ M_s , and the additional plateau phase at $\frac{2}{3}$ M_s —are first-order. In contrast, theory usually predicts second-order transitions to a magnetization-plateau-forming state with gapped low-lying excitations [4, 28]. As has been pointed out by Alicea *et al.* [6], however, one possible explanation of their first order character could be due to the Dzyaloshinskii-Moriya interac-

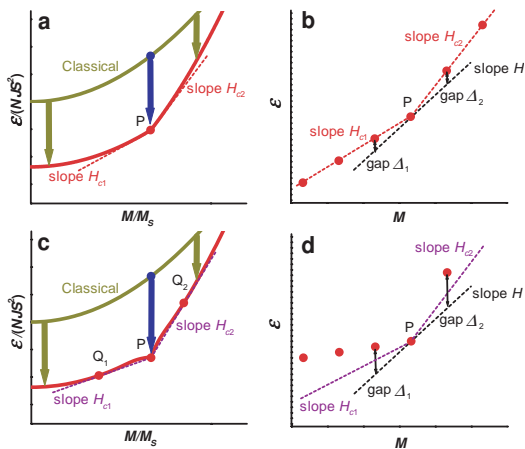


FIG. 3: (Color online) Ground-state energy \mathcal{E} of a frustrated quantum-mechanical Heisenberg antiferromagnet as a function of magnetization M . (a) Macroscopic behavior of $\mathcal{E}(M)$, exhibiting a cusp at a gapped ground state, P. (b) Microscopic, extremely expanded view of the region near P, revealing quantum-mechanically discrete ground states (dots). (c) Macroscopic behavior, when the transitions to state P are first-order. (d) Corresponding microscopic view. In a and c, the magnetic fields are in dimensionless units.

tion, which introduces a cubic term in the free-energy functional.

Here we suggest a new, alternative scenario for consideration. In general, as illustrated in Fig. 3a, when quantum fluctuations select state P as a ground state with energy gaps to the lowest-energy excitations, a cusp must appear in the ground-state energy \mathcal{E} as a function of magnetization M [29]. These excitations are in fact the two ground states adjacent to P, as shown in Fig. 3b. For second-order transitions, the critical fields H_{c1} and H_{c2} are the two derivatives $\partial\mathcal{E}/\partial M$ at P. Over the field range between H_{c1} and H_{c2} (Fig. 3b), P remains the lowest state in the “total” energy $\mathcal{E} - MH$ [30], manifesting itself as a magnetization plateau. When H is either at H_{c1} or H_{c2} , one of the excitations becomes gapless. We speculate, however, that preferential lowering of P by quantum fluctuations might produce inflection points in the vicinity of P, as shown in Fig. 3c. In that case, the lowest total-energy state will change discontinuously at H_{c1} and H_{c2} from P to Q_1 and Q_2 (defined in Fig. 3c). The transitions are now first-order, and are accompanied by non-vanishing energy gaps, as depicted in Fig. 3d. Because this scenario, if verified, relies only on the presence of quantum fluctuations and not the particulars of the spin-orbit interactions in Cs_2CuBr_4 , it would be applicable to a broad range of quantum phase transitions in geometrically frustrated systems.

We thank A. Wilson-Muenchow, T. P. Murphy, J.-H. Park, and G. E. Jones for assistance, and J. Alicea, Y. Fujii, S. Miyahara, and O. Starykh for discussions. This

research was supported by an award from Research Corporation, a Grant-in-Aid for Scientific Research from the JSPS, the Global CEO Program ‘Nanoscience and Quantum Physics’ at Tokyo Tech funded by Monkasho, and the National High Magnetic Field Laboratory (NHMFL) UCGP program and travel grant. The experiments were performed at the NHMFL, which is supported by NSF and the State of Florida. Y.Y. is a JSPS postdoctoral fellow.

* Present address: Institute of Applied Physics and Microstructure Research Center, University of Hamburg, Jungiusstrasse 11, D-20355 Hamburg, Germany.

† Present address: Neutron Scattering Science Division, Oak Ridge National Laboratory, Oak Ridge, TN 37831, USA.

- [1] N. P. Ong and R. J. Cava, *Science* **305**, 52 (2004).
- [2] D. Heidarian and K. Damle, *Phys. Rev. Lett.* **95**, 127206 (2005), and references therein.
- [3] J. E. Greedan, *J. Mater. Chem.* **11**, 37 (2001).
- [4] A. V. Chubukov and D. I. Golosov, *J. Phys.: Condens. Matter* **3**, 69 (1991).
- [5] S. Miyahara, K. Ogino, and H. Furukawa, *Physica B* **378-380**, 587 (2006).
- [6] J. Alicea, A. V. Chubukov and O. A. Starykh, *Phys. Rev. Lett.* **102**, 137201 (2009).
- [7] T. Ono *et al.*, *Phys. Rev. B* **67**, 104431 (2003).
- [8] T. Ono *et al.*, *J. Phys.: Condens. Matter* **16**, S773 (2004).
- [9] T. Ono *et al.*, *J. Phys. Soc. Jpn. Suppl.* **74**, 135 (2005).
- [10] H. Tsujii *et al.*, *Phys. Rev. B* **76**, 060406(R) (2007).
- [11] R. Coldea *et al.*, *Phys. Rev. Lett.* **88**, 137203 (2002).
- [12] S. T. Hannahs and N. A. Fortune, *Physica B* **329-333**, 1586 (2003).
- [13] B. Morosin and E. C. Lingafelter, *Acta Crystallogr.* **13**, 807 (1960).
- [14] U. M. Scheven, S. T. Hannahs, C. Immer, and P. M. Chaikin, *Phys. Rev. B* **56**, 7804 (1997).
- [15] B. Bogenberger *et al.*, *Physica B* **186-188**, 248 (1993).
- [16] B. McCombe and G. Seidel, *Phys. Rev.* **155**, 633 (1967).
- [17] N. Fortune *et al.*, *Rev. Sci. Instrum.* **71**, 3825 (2000).
- [18] Y. Fujii *et al.*, *Physica B* **346-347**, 45 (2004).
- [19] Y. Fujii *et al.*, *J. Phys.: Condens. Matter* **19**, 145237 (2007).
- [20] T. Momoi, H. Sakamoto, and K. Kubo, *Phys. Rev. B* **59**, 9491 (1999).
- [21] E. H. Lieb, T. Schultz, and D. J. Mattis, *Ann. Phys. (N.Y.)* **16**, 407 (1961).
- [22] M. Oshikawa, *Phys. Rev. Lett.* **84**, 1535 (2000).
- [23] G. Misguich, C. Lhuillier, M. Mambrini, and P. Sindzinger, *Eur. Phys. J. B* **26**, 167 (2002).
- [24] M. B. Hastings, *Phys. Rev. B* **69**, 104431 (2004).
- [25] Y. Fujii *et al.*, unpublished.
- [26] S. Miyahara and N. Furukawa, unpublished.
- [27] A. I. Smirnov *et al.*, *Phys. Rev. B* **75**, 134412 (2007).
- [28] K. Damle and T. Senthil, *Phys. Rev. Lett.* **97**, 067202 (2006).
- [29] C. Lhuillier and G. Misguich, in *High Magnetic Fields: Applications in Condensed Matter Physics and Spectroscopy*, edited by C. Berthier, L. P. Lévy, and G. Mar-

tinez (Springer, Berlin, 2002).
[30] In fact the magnetic enthalpy.